communications earth & environment

Article

A Nature Portfolio journal

https://doi.org/10.1038/s43247-025-02730-2

Elevated carbon dioxide does not increase macroalgal community photosynthesis

Shigeki Wada[1,2,3,9] ✉, Shingo Kurosawa[2,4,9], Sylvain Agostini[2,3,5], Ben P. Harvey[2,3], Yuhi Satoh[6], Marco Milazzo[3,7] & Jason M. Hall-Spencer[2,3,8]

Ocean acidification, driven by rising atmospheric carbon dioxide levels, has impacts on marine ecosystems. While elevated carbon dioxide concentrations have the potential to enhance Blue Carbon fixation and storage, the response of community photosynthesis in macroalgal-dominated ecosystems remains poorly understood. Here, we investigated the effects of elevated carbon dioxide on macroalgal communities using volcanic carbon dioxide vents as a natural analogue of ocean acidification. Net community photosynthesis was assessed using chambers positioned on the seafloor as well as water mass dynamics monitoring. Despite a shift in algal community composition, only minimal differences in net community photosynthesis were observed between reference and high carbon dioxide sites. The high carbon dioxide site had a lower abundance of algal species with carbon dioxide concentrating mechanisms, based on $\delta^{13}C$ isotope measurements. Carbon dioxide concentrating mechanisms facilitate photosynthesis under present-day levels of carbon dioxide in seawater, resulting in a negligible effect of elevated carbon dioxide on macroalgal community photosynthesis. These results challenge the assumption that ocean acidification will enhance Blue Carbon uptake and storage, necessitating a reevaluation of this perspective.

The increasing concentration of atmospheric CO_2 is causing changes in the carbonate chemistry of the surface ocean, known as ocean acidification (OA)[1]. This shift can have profound effects on a variety of marine organisms and is expected to alter ecosystem dynamics[2]. One potential consequence of OA is CO_2 fertilization of growth by photosynthetic organisms. The enzyme ribulose 1,5-bisphosphate carboxylase/oxygenase (RuBisCO), responsible for carbon fixation during photosynthesis, is highly sensitive to ambient CO_2 levels[3]. As a result, elevated CO_2 concentrations can enhance photosynthetic activity and could potentially increase carbon storage in marine ecosystems.

Blue Carbon refers to the carbon sequestered by vegetated coastal habitats, and although it has a mitigation potential of less than 2% of current global CO_2 emissions these habitats provide multiple co-benefits[4]. Vascular plants found in soft sediments, such as seagrasses, mangroves, and salt marshes—collectively known as established Blue Carbon habitats—have been the primary focus of research[5]. It is expected that vascular plants in established Blue Carbon habitats will have increased photosynthesis under elevated CO_2 conditions, similar to land plants[6–10]. Consequently, these ecosystems could provide a negative feedback mechanism to climate change[11].

Following suggestions for future Blue Carbon research by Macreadie et al.[12], a wide range of studies on carbon cycling in macroalgal beds have emerged[13,14]. The processes underlying carbon sequestration in macroalgal beds are less understood than for vascular marine plants, despite their high productivity[15]. Export of organic carbon to the deep sea would contribute to carbon sequestration[16,17]. Macroalgae differ fundamentally from vascular plants in their photosynthetic physiology. Some macroalgae have CO_2 concentrating mechanisms (CCMs)[18,19] that allow them to grow in low CO_2 environments, which means their responses to elevated CO_2 may differ from those of vascular plants. To accurately estimate the impact of elevated CO_2 on photosynthesis in macroalgal communities, it is essential to consider potential shifts in species composition. In a high CO_2 world, some species may proliferate, while others may decline[20]. Therefore, it is necessary to assess photosynthetic activity at the community level, focusing on those species that are most successful in a high- CO_2 environment.

[1]Seto Inland Sea Carbon-neutral Research Center, Hiroshima University, Higashi-Hiroshima, Japan. [2]Shimoda Marine Research Center, University of Tsukuba, Shimoda, Japan. [3]Labex ICONA International CO2 Natural Analogues Network, Shimoda, Japan. [4]Yachiyo Engineering CO., Ltd., CS Tower, Taito-ku, Japan. [5]UMR ENTROPIE, IRD, IFREMER, Univ La Réunion, Univ. Nouvelle-Calédonie, Nouméa, New Caledonia. [6]Department of Radioecology, Institute for Environmental Sciences, Rokkasho, Japan. [7]Department of Earth and Marine Sciences, University of Palermo, Palermo, Italy. [8]School of Biological and Marine Sciences, University of Plymouth, Plymouth, UK. [9]These authors contributed equally: Shigeki Wada, Shingo Kurosawa. ✉e-mail: swadasbm@hiroshima-u.ac.jp

Volcanic CO_2 vents provide valuable natural laboratories for studying shifts in benthic community composition[21]. Several studies have documented distinct changes in macroalgal communities across CO_2 gradients[20,22,23]. While an investigation of benthic algal communities in an early successional phase suggested enhanced community photosynthesis under elevated CO_2[24], the response of established macroalgal communities remains poorly understood. Here, we focus on volcanic CO_2 vents off Shikine Island, where changes in macroalgal flora across CO_2 gradients have been well-documented[23,25,26]. To evaluate community photosynthesis, we used two experimental approaches: using chambers to enclose the seafloor (Experiment 1)[27,28] and monitoring water mass dynamics (Experiment 2)[29]. Additionally, we assessed the performance of CCM by analysing carbon isotope ratios ($\delta^{13}C$), which reveal physiological processes involved in CO_2 uptake. We used these techniques at a natural analogue for ocean acidification to investigate how community photosynthesis was affected by shifts in species composition and physiological traits related to CO_2 uptake.

Results

Chamber experiment (Experiment 1)

Seawater pH at our high CO_2 site was significantly lower than at our reference site ($p < 0.001$), with differences ranging from 0.10 to 0.33 pH units (Supplementary Fig. 1a). Partial pressure of CO_2 (pCO_2) levels ranged 292–391 µatm at the reference site and 509–909 µatm at the high CO_2 site (Supplementary Fig. 1b). The differences in temperature were within 1 °C (0.14–0.83 °C) in most surveys except for two occasions (high CO_2 and reference site in January (13.9 and 10.1 °C) and February (16.8 and 15.1 °C), respectively) (Supplementary Fig. 1c). Salinity and alkalinity levels were also similar between sites, ranging from 33.5–34.7 to 2230–2290 µmol kg^{-1}, respectively, with no significant differences observed (Supplementary Fig. 1d, e). These findings align with carbonate chemistry data from previous studies conducted at these same locations[23].

Seasonal variations in algal communities around Shikine Island are strongly affected by the impacts of the typhoon season that can remove macroalgal biomass. Therefore, rather than grouping the survey by temperature, the data were grouped according to the typhoon season. These were categorized as Pre (April, June, September), Post (November, December), and Recovery (January, February) according to Hudson et al.[26]. Algal communities on shallow coastal bedrock at 4–8 m depth below Chart Datum significantly differed between reference and high CO_2 sites. At the reference site, *Gelidium elegans* (Pre: 15.3 ± 4.4, Post: 15.8 ± 4.0 and Recovery: 17.3 ± 5.0% cover; mean ± SE, n = 15-30) and coralline algae (crustose in Pre: 11.5 ± 2.7, Post: 20.3 ± 3.2 and Recovery: 11.6 ± 2.7% cover, branched in Pre: 13.3 ± 3.2, Post: 34.0 ± 6.3 and Recovery: 11.5 ± 3.6% cover, n = 15-30) predominated ($p < 0.01$). In contrast, *Zonaria diesingiana* was at the high CO_2 site (Pre: 31.7 ± 4.5, Post: 56.5 ± 5.0 and Recovery: 59.1 ± 6.6% of substratum cover, n = 15-28, $p < 0.01$) (Supplementary Fig. 2a).

We carried out functional group analysis similar to Agostini et al.[23] revealing higher cover of coralline algae (crustose and branched) and canopy-forming algae, including *G. elegans* ($p < 0.01$), at the reference site. Conversely, algae with small erect thalli, which we grouped as low-profile algae, such as *Z. diesingiana*, were more dominant at the high CO_2 site ($p < 0.01$). Turf algae were observed exclusively at the high CO_2 site during the Pre typhoon season, with significantly greater cover than at the reference site ($p < 0.001$) (Supplementary Fig. 2a). These findings are consistent with previous research[23,25,26,30]. The five dominant functional groups—crustose coralline algae (CCA), branched coralline algae (BCA), canopy-forming algae, low-profile algae, and turf algae—collectively covered 73–92% of the rocky seafloor (Fig. 1a). Community composition differed significantly between sites, as indicated by PERMANOVA (Permutational Multivariate Analysis of Variance) ($p < 0.001$, Supplementary Table 1) and nMDS (non-metric Multidimensional Scaling) analyses (Supplementary Fig. 2b). On the contrary to community composition, shift of biomass (dry weight) between reference and high CO_2 sites was unclear (two-way ANOVA, $p = 0.083$) (Supplementary Fig. 2c, Supplementary Table 2).

At the reference site, Net Community Photosynthesis (NCP) values were 313 ± 79, 112 ± 50, and 432 ± 90 mg O_2 m^{-2} h^{-1}, while at the high CO_2 site, they were 181 ± 67, 159 ± 29, and 557 ± 57 mg O_2 m^{-2} h^{-1} ($n = 10$–31) during the Pre, Post, and Recovery seasons, respectively (Supplementary Fig. 3). Solar irradiance ranged 75–500 (338 ± 45, 155 ± 37 and 191 ± 26 in Pre, Post and Recovery Seasons, respectively; mean ± se) and 4.8-560 (264 ± 41, 152 ± 21 and 206 ± 22 in Pre, Post, Recovery Seasons, respectively) µmol photon m^{-2} s^{-1} at reference and high CO_2 sites, respectively. Given the dependence of photosynthesis on solar radiation, a two-way linear mixed model was employed to assess light-normalized photosynthesis between sites, with Light, Temperature and Site as fixed factors and Season as a random factor. The linear relationship between NCP and light intensity in the chamber experiments suggests that light levels were below the saturation point, with the slope of the regression line representing the initial slope of the photosynthesis-irradiance curve (Fig. 2). NCP showed a significant positive correlation with Light ($p < 0.0001$) and Temperature ($p < 0.001$); however, no significant differences were observed between sites ($p = 0.614$) (Table 1) without any interaction among the fixed factors. We also tested the relationship between NCP normalized by total weight of algal biomass (NCPw) and Light, but no significant correlation was found ($p = 0.142$) (Supplementary Fig. 4, Supplementary Table 3). The light-normalized slope values for NCP in each site were calculated using a one-way linear mixed model (LMM, fixed factor: Light, random factor: Season), yielding 0.359 ± 0.039 and 0.333 ± 0.047 mg O_2 $photons^{-1}$ for the reference and high CO_2 sites, respectively.

Monitoring water mass dynamics (Experiment 2)

The pH in total scale at our high CO_2 site was significantly lower (7.53 ± 0.06 (7.35–7.66), mean ± SD, n = 1,440) compared to our reference site (8.05 ± 0.03 (8.01–8.12) $n = 3,240$; Supplementary Fig. 5a, b). Temperature and solar irradiance were similar between sites, with temperature ranging 23.6–25.4 °C at the reference site and 21.4–25.6 °C at the high CO_2 site (Supplementary Fig. 5c, d). Solar irradiance ranged from 0-551 at the reference site and 0–477 µmol photon m^{-2} s^{-1} at the high CO_2 site (Supplementary Fig. 5e, f). At the reference site, canopy-forming and coralline algae were prevalent, while the high CO_2 site was more dominated by turf algae (Supplementary Fig. 6). $NCP_{\Delta DO}$ (NCP measured in Experiment 2: see methods and Supplementary Information) values ranged from −0.10 to 0.13 g O_2 min^{-1} at the reference site and −0.014 to 0.092 g O_2 min^{-1} at the high CO_2 site. $NCP_{\Delta DO}$ was positively correlated with solar irradiance ($p < 0.001$; Fig. 3, Table 2). No significant difference was found for the slopes of the $NCP_{\Delta DO}$ versus solar irradiance between the sites ($p = 0.585$; Table 2).

Carbon concentrating mechanism performance based on ^{13}C analysis

The $\delta^{13}C$ values of algal samples ranged from −7.30 to −31.7‰ (Supplementary Table 4), which is an indicator of CCM. $\delta^{13}C$ value of HCO_3^- is higher than that of CO_2 due to isotopic disequilibrium. Since one of the important processes of CCM is conversion of HCO_3^- to CO_2 with carbonic anhydrase, macroalgae were classified into three groups following Velazquez-Ochoa et al.[31]: CCM users (values higher than −10‰), both CCM and diffusive CO_2 users (values between −11 and −30‰), and non-CCM users (values lower than −30‰). Species with $\delta^{13}C$ values higher than −10‰, including coralline algae and the green alga *Codium lucasii*, were predominantly collected from the reference site. Non-CCM users, such as *Neorhodomela aculeata*, which had $\delta^{13}C$ values lower than −30‰, were exclusively collected from the high CO_2 site during the Pre typhoon season. Seven species were present at both sites, and their $\delta^{13}C$ values were significantly higher at the reference site ($p < 0.001$; Supplementary Table 5), indicating intraspecific plasticity in CCM performance relative to ambient CO_2 concentrations.

At the reference site, $\Sigma^{13}C$ values ranged from −17.5 to −12.5 during the Pre typhoon season and −17.4 to −9.12 during the Post season, significantly higher than those at the high CO_2 site, which ranged from −20.8 to −13.6 and −19.5 to −12.5‰ during the Pre and Post seasons, respectively ($p < 0.001$;

Fig. 4). Although $\Sigma^{13}C$ values at the reference site tended to be higher during the Recovery season, the difference between sites was not statistically significant.

Discussion

In this study, we investigated Net Community Photosynthesis in response to ocean acidification using volcanic CO_2 vents, which serve as a natural laboratory capable of addressing ecosystem-level complexities. Areas with different levels of CO_2 had distinct macroalgal communities with coralline algae (both branched and crustose) and canopy-forming algae dominant at the reference site, while low-profile and turf algae were dominant at the high CO_2 site. These shifts in community composition observed with the elevation of CO_2 are consistent with previous studies of benthic communities along CO_2 gradients around Shikine Island[23,25,26,30]. Estimates of NCP using two independent methods in the present study show that increased CO_2 levels had a negligible effect on macroalgal community production, challenging the notion that photosynthetic growth might be boosted as the availability of carbon increases.

The response of macroalgae to OA relates to physiological processes underlying CO_2 fixation. If we consider only the affinity of RuBisCO for CO_2, photosynthesis might be expected to increase under OA, since current CO_2 concentrations in the ocean (approximately 300–400 ppm) are generally below the half-saturation constant of RuBisCO (approximately 50 μM)[32]. However, the majority of macroalgal species would have C3 process plus CCM[33] with a few exceptional cases[34], suggesting that photosynthesis could be enhanced at the current CO_2 concentrations[35]. Some macroalgal species may exhibit intraspecific plasticity in their CCM performance to optimize their survival strategy depending on ambient CO_2

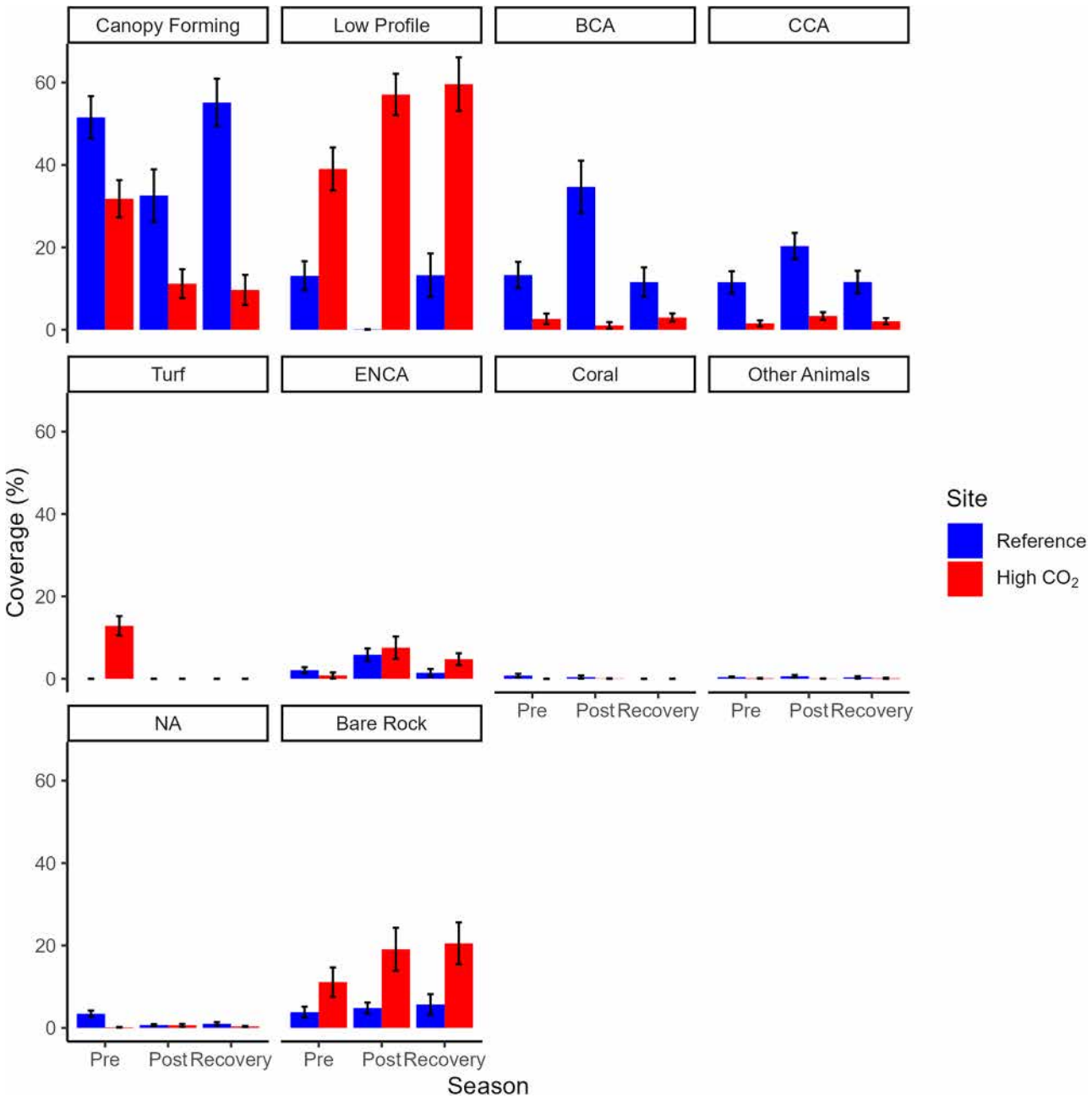

Fig. 1 | Coverage of macroalgal functional groups in a benthic chamber experiment at two sites off Shikine Island, Japan. Error bars show SE (Reference: $n = 30$, 22 and 15, High CO_2: $n = 28$ 19 and 16 in Pre, Post and Recovery Seasons, respectively). BCA, CCA, ENCA, and NA indicate Branched Coralline Algae, Crustose Coralline Algae, Encrusting Non Calcifying Algae and Not Applicable, respectively.

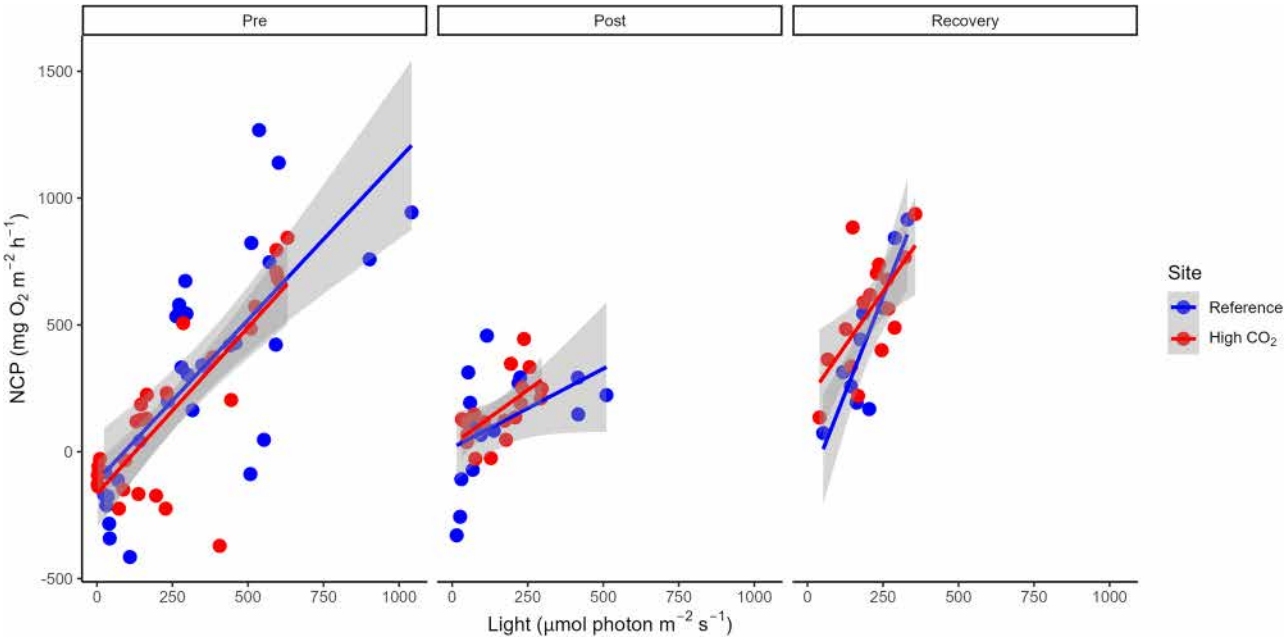

Fig. 2 | Correlation between Net Community Photosynthesis and Light in benthic chambers before a typhoon season, after and during the recovery of macroalgal communities off Shikine Island, Japan. Shadings imply 95% confidence intervals. Ordinate and abscissa indicate NCP and light intensity, respectively.

Table 1 | Results of linear mixed model in the Experiment 1

	Numerator df	Denominator df	F	*P*
Intercept	1	111	18.8	<0.001
Light	1	111	136	<0.001
Site	1	111	0.256	0.614
Temp	1	111	12.3	<0.001
Light × Site	1	115	0.0012	0.973
Light × Temp	1	111	0.0041	0.949
Site × Temp	1	111	0.0041	0.949
Light × Site × Temp	1	111	1.92	0.168

Explanatory variables, light, temperature and site, and interaction between them are shown.

concentrations[36]. Moreover, species without CCM (or low-affinity CCM) could be benefited under high CO_2[18]. Therefore, interspecific differences in CCM performance must also be considered, as shifts in community composition are expected under OA[20,23].

The small variability in NCP despite changes in CO_2 concentration may be related to both intraspecific plasticity and interspecific differences in the physiological processes involved in CO_2 fixation. Seven macroalgal species collected from reference and high CO_2 sites showed down regulation of CCM at the high CO_2 site (Supplementary Table 5). Additionally, shifts in species composition could affect CCM performance at the community level. Species showing active CCM usage were predominantly found at the reference site, while species that rely on dissolved CO_2 (non-CCM users) were exclusive to the high CO_2 site (Supplementary Table 4). The performance of CCM at the community level was assessed by calculating $\Sigma^{13}C$, which was consistently higher in the reference site (Fig. 4), showing a higher contribution of CCM, compared to the high CO_2 site. This is in line with previous research suggesting that macroalgae with lower $\delta^{13}C$ values dominate high CO_2 environments around other volcanic CO_2 vents (e.g. Vulcano and Ischia Islands, Italy)[18], and that reduced CCM performance under high CO_2 conditions is a general response to OA. Our results imply that macroalgae with less CCM performance have an advantage to survive under high CO_2 environment probably due to saving energy cost in CCM processes. Balance between CO_2 availability and energy cost for CCM would be a key factor determining macroalgal ecosystem dynamics.

While CO_2 fertilization in coastal vegetated ecosystems, such as seagrass beds, mangrove forests, and salt marshes, is expected to enhance Blue Carbon capacity[6–10] and provide negative feedback on climate change[11], the response of macroalgal NCP remains unclear, despite their high productivity[15]. Most macroalgae possess CCM[33] unlike land plants[37], which likely allow them to adapt to current CO_2 levels, reducing carbon limitation for their photosynthesis. Combined with major changes in the macroalgal communities with low CCM performance driven by high CO_2, our study suggests that ocean acidification will have a negligible effect on macroalgal net community photosynthesis.

Analysis of carbon sequestration from macroalgal-dominated ecosystems has only recently begun. Our results reveal a negligible effect of elevated CO_2 on macroalgal NCP, suggesting that potential for CO_2 fertilization to enhance Blue Carbon in macroalgal systems should be reconsidered. Carbon fixation is the start of the process underlying Blue Carbon, but it is not equal to sequestration as much of the carbon produced by macroalgae is labile and will not be permanently stored. Organic matter derived from macroalgae can by exported and sequestered into the deep sea after dislodgement[17,38]. Therefore, a variety of processes such as export, decomposition and sinking are relevant to Blue Carbon. Although knowledge on the effect of elevated CO_2 on these processes in fate of macroalgal organic matter is still limited, an increase in export flux of algal biomass under high CO_2 was suggested in a previous study carried out across CO_2 gradient around Shikine Island[24]. To predict the feedback of macroalgal systems for climate change, the impact of elevated CO_2 on those processes in the fate of organic matter should be highlighted.

Methods

Net community photosynthesis estimates using a chamber experiment (Experiment 1)

Experiment 1 was conducted at two locations: a high CO_2 site, situated near a CO_2 vent in Mikawa Bay on Shikine Island (139.2°N, 34.3°E; Supplementary Fig. 7a, b), Japan, and a reference site, located in another bay

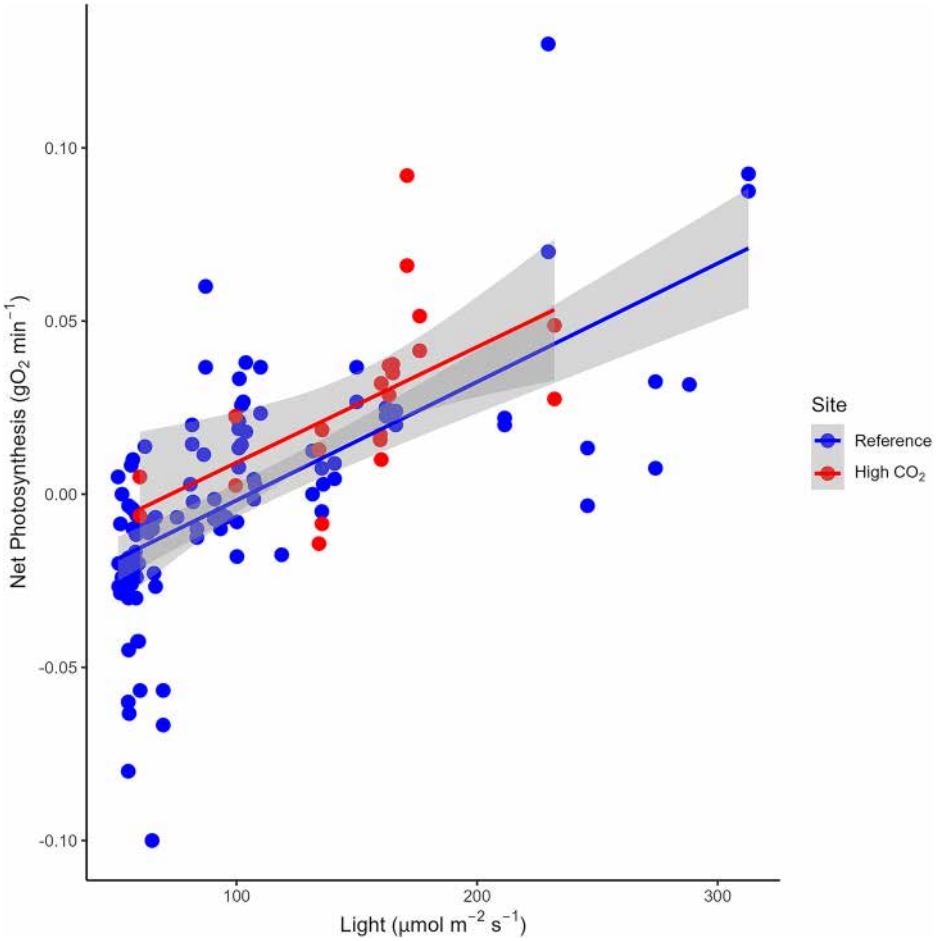

Fig. 3 | Correlation between net community photosynthesis $_{\Delta DO}$ and light during water mass dynamic monitoring at 8–10 m depth off Shikine Island, Japan. Shadings imply 95% confidence intervals.

Table 2 | Results of analysis of covariance (ANCOVA) for $NCP_{\Delta DO}$ during water mass dynamic monitoring at 8–10 m depth off Shikine Island, Japan

	Estimate	SE	t value	*p*
Intercept	-3.50×10^{-2}	0.49×10^{-2}	7.19	<0.001
Light	3.36×10^{-4}	0.39×10^{-4}	8.72	<0.001
Site	1.07×10^{-2}	1.95×10^{-2}	0.55	0.585
Light × Site	-1.90×10^{-6}	127×10^{-6}	−0.02	0.988

Explanatory variables, light and site, and interaction between them are shown.

outside the influence of the vent (Supplementary Fig. 7c). Surveys were conducted on eight occasions across various seasons (June, November, and December 2017; January, February, April, June, and September 2018). The experimental chambers used in the experiment had a truncated cone shape, constructed from a metal frame and transparent plastic sheet. The chambers measured 25 cm and 20 cm in diameter at the base and top, respectively, with a height of 16.5 cm. A plastic skirt extended from the chamber's edge, weighted with beads to ensure proper sealing against the seafloor (Supplementary Fig. 8). Each chamber had a dissolved oxygen and temperature meter connected to a logger (Multi 3410, WTW) on a floating buoy to continuously monitor dissolved oxygen (DO) concentrations at 5 s intervals.

A circular area (25 cm in diameter, matching the chamber base) was randomly marked on the seafloor, and then photographed, before placing the chamber in the same location. These photographs were used to estimate floral coverage following Agostini et al.[17]. A photometer (DEFI-L, JFE-ADVANTEC) placed adjacent to the chamber measured solar irradiance at 1 s intervals to calculate mean light levels in each incubation period. Water within the chambers was gently mixed by agitating oxygen probe attached with the chamber through the 10-minute incubation to ensure uniform oxygen concentrations. After incubation, 2 ml of diluted fluorescent dye (Bright Dyes, Fluorescent FLT Yellow/Green) was injected into the chamber, and seawater was retrieved to calculate the chamber's water volume via dilution rates. Fluorescence intensity was measured using a fluorophotometer (F-7000, Hitachi) at excitation and emission wavelengths of 490 nm and 515 nm, respectively. We confirmed the linearity of fluorescence intensity across a dilution range from 500,000 to 4,000,000 (Dilution rate: $0.25–2.0 \times 10^{-6}$, Supplementary Fig. 9). DO changes over time (Supplementary Fig. 10) were analyzed using linear regression, and NCP was calculated from the slope of DO concentration versus time using the equation:

$$\mathrm{NCP} = S \times V / A \quad (1)$$

where S represents the slope of DO change (mg O_2 $l\text{-}1^{-1}$ h^{-1}), V is the water volume (l), and A is the area of the chamber bottom (m^2).

Seawater samples were collected by SCUBA divers near the experimental sites. Water salinity and pH (on the total scale) were measured using a portable multi-sensor (Orion Star A329, ThermoFisher Scientific) within a few hours after collection. Seawater samples were filtered through disposable membrane filters (DISMIC-25AS, ADVANTEC), and the total alkalinity of the filtrate was then measured using an auto-titrator (916 Ti-Touch, Metrohm)[30].

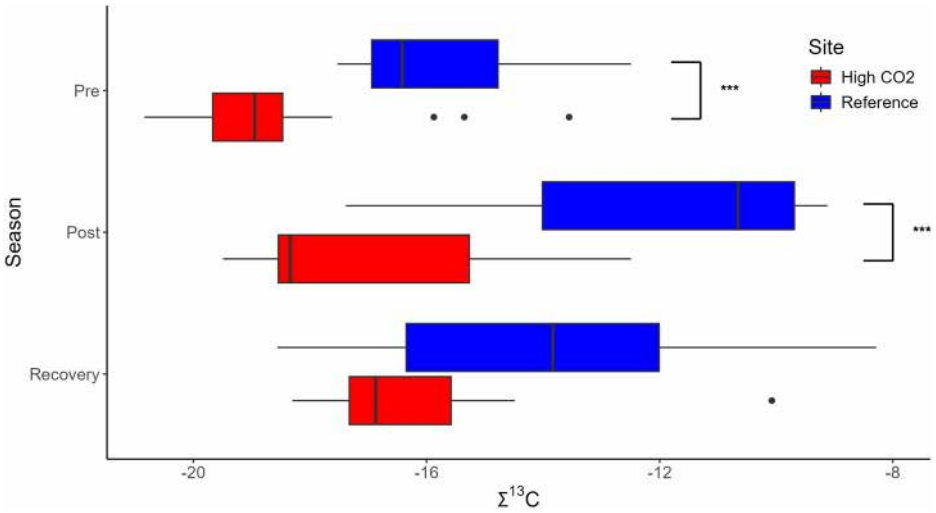

Fig. 4 | Variation in $\Sigma^{13}C$ values before a typhoon season, then after and during a period of macroalgal community recovery. Asterisks (***) show significant differences ($p < 0.001$).

Net community photosynthesis estimates by monitoring water mass dynamics (Experiment 2)

Experiment 2 was conducted near the chamber experiment site (Supplementary Fig. 7b, c) in October 2018. Sensors were deployed in a 400 m^2 area (20 × 20 m) at both high- CO_2 and reference sites for two days. Oxygen sensors were positioned at the square's corners, while temperature- and pH (in total scale)- (MX-2501, ONSET HOBO), current- (INFINITY-EM, JFE-ADVANTEC) and photo-meters (DEFI-L, JFE-ADVANTEC) were placed centrally. Data were logged at 1 min intervals. Horizontal water mass transport was estimated from current measurements, and net community photosynthesis ($NCP_{\Delta DO}$) was calculated by dividing oxygen concentration changes by the water mass travel duration. The position of certain water mass was traced according to the horizontal current. In case that the coordinate of the water mass at certain corner reached in the area within 2 m from other corners, the change in DO concentration was logged to calculate $NCP_{\Delta DO}$. Since the location of the study area is nearby coastline, the reflection of water current could bring serious error in the analysis. In the high CO_2 site, the location was close the coastline on the northern side (Supplementary Fig. 7b). Therefore, the directions of the export toward east and west were used. Since the location in the reference site is inside of a bay (Supplementary Fig. 7c), we only used the direction of the export of water mass toward outside. The duration of the export of water mass was limited in the range from 10 to 100 min. The experiment was carried out for 3 days (from 14th to 16th October in control and 10th to 12th October in high CO_2 sites), and the datasets in daytime (solar irradiance >50 µmol photon m^{-2} s^{-1}) were used. These estimates provide relative site comparisons, as vertical diffusion was not evaluated. Therefore, it is difficult to directly compare the results in experiments 1 and 2 due to the difference in the unit. Benthic functional group coverage was estimated using random seafloor photography within 50 × 50 cm quadrats, analysed following Steneck and Dethier[39].

Analysis of ^{13}C

Benthic flora, excluding crustose coralline algae, were collected by hand (at random) nearby the area of Experiment 1. Samples of each species were dried at 60 °C, ground into fine powder, and treated with vapor-phase HCl in a desiccator for 24 h to remove inorganic carbon. Stable isotope analysis was performed using an elemental analyzer/isotope ratio mass spectrometer (EA/IRMS) (ThermoFisher, Delta V). To evaluate CCM performance at the community level, the average $\delta^{13}C$ values of each functional group, site, and season were weighted by their respective coverages to calculate $\Sigma^{13}C$ using the equation:

$$\Sigma^{13}C = C_1 \times \delta^{13}C_1 + C_2 \times \delta^{13}C_2 \ldots C_n \times \delta^{13}C_n \quad (2)$$

where C_k and $\delta^{13}C_k$ represent the coverage and $\delta^{13}C$ values of a specific functional group k, respectively. For $\Sigma^{13}C$ calculations, data from BCA, Canopy-Forming Algae, Low-Profile Algae, and Encrusting Non-Calcifying Algae were used. Since $\delta^{13}C$ values for CCA were not measured, values for BCA were used as substitutes.

Statistical analysis

Water chemistry parameters (pH in total scale, temperature, salinity, and alkalinity) were analyzed using a two-way ANOVA with season and site as factors. Taxonomic and functional group differences were compared individually using the Wilcoxon rank sum test (Bonferroni-adjusted). Changes in community composition were assessed using PERMANOVA and nMDS analyses based on Bray Curtis distance with the 'vegan' package[40]. Shift of biomass (dry weight) per community area was tested with two-way ANOVA with factors of Site and Season. NCP from Experiment 1 was analyzed using a three-way LMM (fixed factors: Light, Temperature and Site, random factor: Season) with the 'nlme' package[41]. The slope of NCP versus Light at each site was calculated using a one-way LMM (fixed factor: Light, random factor: Season). $NCP_{\Delta DO}$ from Experiment 2 was analyzed using analysis of covariance (ANCOVA) with Light and Site as factors. Intraspecific $\delta^{13}C$ differences were evaluated using 3-way ANOVA with Season, Site and Species as factors. Community-normalized $\delta^{13}C$ ($\Sigma^{13}C$) was compared using the Wilcoxon rank sum test (Bonferroni-adjusted). For these tests, we used the program R version 4.3.1.

Reporting summary

Further information on research design is available in the Nature Portfolio Reporting Summary linked to this article.

Data availability

All data are uploaded upon Zenodo. https://doi.org/10.5281/zenodo.16653946.

Code availability

All R code are uploaded upon Zenodo. https://doi.org/10.5281/zenodo.16653946.

Received: 16 April 2025; Accepted: 21 August 2025;
Published online: 31 October 2025

References

1. Ma, D., Gregor, L. & Gruber, N. Four decades of trends and drivers of global surface ocean acidification. *Glob. Biogeochem. Cycles* **37**, e2023GB007765 (2023).

2. Doney, S. C., Busch, D. S., Cooley, S. R. & Kroeker, K. J. The impacts of ocean acidification on marine ecosystems and reliant human communities. *Annu. Rev. Environ. Resour.* **45**, 83–112 (2020).
3. Israel, A. & Hophy, M. Growth, photosynthetic properties and Rubisco activities and amounts of marine macroalgae grown under current and elevated seawater CO_2 concentrations. *Glob. Change Biol.* **8**, 831–840 (2002).
4. Intergovernmental Panel On Climate Change (IPCC). *The Ocean and Cryosphere in a Changing Climate: Special Report of the Intergovernmental Panel on Climate Change*. (Cambridge University Press,) https://doi.org/10.1017/9781009157964 (2022).
5. *Blue Carbon: The Role of Healthy Oceans in Binding Carbon: A Rapid Response Assessment*. (Arendal, Norway, 2009).
6. Farnsworth, E. J., Ellison, A. M. & Gong, W. K. Elevated CO_2 alters anatomy, physiology, growth, and reproduction of red mangrove (*Rhizophora mangle* L.). *Oecologia* **108**, 599–609 (1996).
7. Jacotot, A., Marchand, C., Gensous, S. & Allenbach, M. Effects of elevated atmospheric CO_2 and increased tidal flooding on leaf gas-exchange parameters of two common mangrove species: *Avicennia marina* and *Rhizophora stylosa*. *Photosynth. Res.* **138**, 249–260 (2018).
8. Jacotot, A., Marchand, C. & Allenbach, M. Increase in growth and alteration of C:N Ratios of *Avicennia marina* and *Rhizophora stylosa* subject to elevated CO_2 concentrations and longer tidal flooding duration. *Front. Ecol. Evol.* **7**, 98 (2019).
9. Apostolaki, E. T., Vizzini, S., Hendriks, I. E. & Olsen, Y. S. Seagrass ecosystem response to long-term high CO_2 in a Mediterranean volcanic vent. *Mar. Environ. Res.* **99**, 9–15 (2014).
10. Berlinghof, J. et al. The role of epiphytes in seagrass productivity under ocean acidification. *Sci. Rep.* **12**, 6249 (2022).
11. Mo, Y., Kearney, M. S. & Turner, R. E. Feedback of coastal marshes to climate change: Long-term phenological shifts. *Ecol. Evol.* **9**, 6785–6797 (2019).
12. Macreadie, P. I. et al. The future of Blue Carbon science. *Nat. Commun.* **10**, 3998 (2019).
13. Krause-Jensen, D. & Duarte, C. Substantial role of macroalgae in marine carbon sequestration. *Nat. Geosci.* **9**, 737–742 (2016).
14. Krause-Jensen, D. et al. Sequestration of macroalgal carbon: the elephant in the Blue Carbon room. *Biol. Lett.* **14**, 20180236 (2018).
15. Duarte, C. M. et al. Global estimates of the extent and production of macroalgal forests. *Glob. Ecol. Biogeogr.* **31**, 1422–1439 (2022).
16. Ortega, A. et al. Important contribution of macroalgae to oceanic carbon sequestration. *Nat. Geosci.* **12**, 748–754 (2019).
17. Filbee-Dexter, K. et al. Carbon export from seaweed forests to deep ocean sinks. *Nat. Geosci.* **17**, 552–559 (2024).
18. Cornwall, C. E. et al. Inorganic carbon physiology underpins macroalgal responses to elevated CO_2. *Sci. Rep*. **7**, 46297 (2017).
19. Raven, J. A., Beardall, J. & Sánchez-Baracaldo, P.3. The possible evolution and future of CO_2-concentrating mechanisms. *J. Exp. Bot.* **68**, 3701–3716 (2017).
20. Porzio, L., Buia, M. C. & Hall-Spencer, J. M. Effects of ocean acidification on macroalgal communities. *J. Exp. Mar. Biol. Ecol.* **400**, 278–287 (2011).
21. Hall-Spencer, J. M. et al. Volcanic carbon dioxide vents show ecosystem effects of ocean acidification. *Nature* **454**, 96–99 (2008).
22. Baggini, C. et al. Seasonality Affects Macroalgal Community Response to Increases in pCO_2. *PLOS ONE* **9**, e106520 (2014).
23. Agostini, S. et al. Ocean acidification drives community shifts towards simplified non-calcified habitats in a subtropical−temperate transition zone. *Sci. Rep*. **8**, 11354 (2018).
24. Wada, S., Agostini, S., Harvey, B. P., Omori, Y. & Hall-Spencer, J. M. Ocean acidification increases phytobenthic carbon fixation and export in a warm-temperate system. *Estuar. Coast. Shelf Sci.* **250**, 107113 (2021).
25. Cattano, C. et al. Changes in fish communities due to benthic habitat shifts under ocean acidification conditions. *Sci. Total Environ.* **725**, 138501 (2020).
26. Hudson, C. J. et al. Ocean acidification increases the impact of typhoons on algal communities. *Sci. Total Environ.* **865**, 161269 (2023).
27. Ishikawa, Y., Fujimura, H. & Suzuki, Y. Closed-chamber system for primary production of benthic communities in sub-tropical lagoon. *Eco-Eng.* **19**, 173–177 (2007).
28. Reis, B. et al. Benthic Incubation Chamber (BIC) for in-situ assessment of primary productivity in different canopy-forming communities. *Mar. Biol.* **171**, 178 (2024).
29. Falter, J. L., Lowe, R. J., Atkinson, M. J., Monismith, S. G. & Schar, D. W. Continuous measurements of net production over a shallow reef community using a modified Eulerian approach. *J. Geophys. Res. Oceans* **113**, 2007JC004663 (2008).
30. Harvey, B. P. et al. Feedback mechanisms stabilise degraded turf algal systems at a CO_2 seep site. *Commun. Biol.* **4**, 1–10 (2021).
31. Velázquez-Ochoa, R., Ochoa-Izaguirre, M. J. & Soto-Jiménez, M. F. An analysis of the variability in $\delta^{13}C$ in macroalgae from the Gulf of California: indicative of carbon concentration mechanisms and isotope discrimination during carbon assimilation. *Biogeosciences* **19**, 1–27 (2022).
32. Koch, M., Bowes, G., Ross, C. & Zhang, X. Climate change and ocean acidification effects on seagrasses and marine macroalgae. *Glob. Change Biol.* **19**, 103–132 (2013).
33. Sand-Jenscn, K. & Gordon, D. M. Differential ability of marine and freshwater macrophytes to utilize HCO_3^- and CO_2. *Mar. Biol.* **80**, 247–253 (1984).
34. Liu, D. et al. Role of C4 carbon fixation in Ulva prolifera, the macroalga responsible for the world's largest green tides. *Commun. Biol.* **3**, 494 (2020).
35. Wu, H., Zou, D. & Gao, K. Impacts of increased atmospheric CO_2 concentration on photosynthesis and growth of micro- and macro-algae. *Sci. China C. Life Sci.* **51**, 1144–1150 (2008).
36. Van Der Loos, L. M. et al. Responses of macroalgae to CO_2 enrichment cannot be inferred solely from their inorganic carbon uptake strategy. *Ecol. Evol.* **9**, 125–140 (2019).
37. Raven, J. A., Ball, L. A., Beardall, J., Giordano, M. & Maberly, S. C. Algae lacking carbon-concentrating mechanisms. *Can. J. Bot.* **83**, 879–890 (2005).
38. Pessarrodona, A. et al. Carbon sequestration and climate change mitigation using macroalgae: a state of knowledge review. *Biol. Rev.* **98**, 1945–1971 (2023).
39. Steneck, R. S. & Dethier, M. N. A Functional Group Approach to the Structure of Algal-Dominated Communities. *Oikos* **69**, 476 (1994).
40. Oksanen, J. et al. Vegan: Community Ecology Package. R package version 2.5-6 (2019)
41. Pinheiro, J. et al. nlme: Linear and Nonlinear Mixed Effects Models. R package version 3.1-149 (2020).

Acknowledgements

We thanks the technical staffs of Shimoda Marine Research Center and Mr. Yasutaka Tsuchiya, for help with field sampling. We are also grateful to Drs. H. Fujimura and T. Hama for his kind advice. The field survey was permitted by Nii-jima Fishery Cooperatives Shikine-jima Branch. This study was supported by the Environment Research and Technology Development Fund (4RF-1701), the Ministry of Education, Science, Sports and Culture, Grant-in-Aid for Scientific Research (B) (19H04234) and (A) (22H00555), and International CO2 Natural Analogues (ICONA) Network supported by JSPS Core-to-Core Program (JPJSCCA20210006). This study is a contribution to the Scientific Committee on Oceanic Research *Changing Oceans Biological Systems* project (OCE-1840868).

Author contributions

S.W. and S.A. designed the study. S.W., S.K., S.A., B.P.H., M.M., and J.M.H-P. carried out field survey. S.W., S.K., and Y.S. performed stable isotope analysis. The analysis of main results was performed by S.W., S.K., S.A., B.P.H. All authors contributed to editing and discussion of the paper.

Competing interests

The authors declare no competing interest.

Additional information

Supplementary information The online version contains supplementary material available at https://doi.org/10.1038/s43247-025-02730-2.

Correspondence and requests for materials should be addressed to Shigeki Wada.

Peer review information *Communications Earth and Environment* thanks Peng Jin, Futian Li for their contribution to the peer review of this work. Peer review was single-anonymous OR Peer review was double-anonymous. Primary Handling Editor: Alice Drinkwater. A peer review file is available.